Available online at www.sciencedirect.com

SciVerse ScienceDirect

Ceramics International 39 (2013) 5689–5694

CERAMICS INTERNATIONAL

www.elsevier.com/locate/ceramint

Structure and electrical properties of $[(K_{0.49}Na_{0.51})_{1-x}Li_x](Nb_{0.90}Ta_{0.04}Sb_{0.06})O_3$ lead-free piezoceramics

Haiwei Du[a,b], Yanqiu Huang[a,b,*], Hongping Tang[a,b], Wei Feng[a,b], Haina Qin[a,b], Xiufang Lu[a,b]

[a]Faculty of Materials Science and Chemistry, China University of Geosciences, Wuhan 430074, PR China
[b]Engineering Research Center of Nano-Geomaterials of Ministry of Education, China University of Geosciences, Wuhan 430074, PR China

Received 27 November 2012; received in revised form 25 December 2012; accepted 25 December 2012
Available online 3 January 2013

Abstract

Lead-free $[(K_{0.49}Na_{0.51})_{1-x}Li_x](Nb_{0.90}Ta_{0.04}Sb_{0.06})O_3$ (KNLNTS) ceramics were prepared by a conventional ceramic processing method, and the effects of Li content on the crystal phases and electrical properties of the ceramics were investigated. A secondary phase was identified by XRD analysis when $x=0.08$, indicating that the maximum solid solubility of lithium in KNLNTS solid solutions is lower than 8 mol%. The Curie temperature T_C increased while the polymorphic phase transition (PPT) temperature T_{O-T} decreased with the increasing Li content. The coexistence of orthorhombic and tetragonal phases was observed near room temperature when $x=0.04$. The optimum electrical performance, i.e. piezoelectric coefficient $d_{33}=215$ pC/N, electromechanical coupling coefficient $k_p=0.313$, $k_t=0.306$, relative permittivity $\varepsilon_{33}^T/\varepsilon_0=805$ and loss tangent tan $\delta=0.045$, was obtained for $x=0.04$.

Keywords: C. Dielectric properties; C. Piezoelectric properties; Ceramics; Phase transition

1. Introduction

Potassium sodium niobate ($K_{0.5}Na_{0.5}NbO_3$, abbreviated as KNN) is a well known lead-free piezoelectric material, which has a high Curie temperature ($T_C\sim420$ °C) and promising piezoelectric properties [1]. However, the pure KNN ceramics are very difficult to densify by the traditional sintering processes because of the volatility of alkaline components and the low phase stability at high temperatures [2]. In order to improve the densification and the electrical properties of the KNN ceramics, many KNN-based systems have been investigated. It is found that the ternary system $(K,Na)NbO_3$–$LiTaO_3$–$LiSbO_3$ exhibits excellent piezoelectric properties [3]. The investigation of the orthorhombic–tetragonal polymorphic phase transition (PPT) of the KNN-based ceramics reveals that the PPT temperature (T_{O-T}) is obviously affected by the added elements. Many researchers have shown that the T_{O-T} of the KNN-based ceramics is shifted to low temperature by adding some elements or compounds, and the piezoelectric properties of the ceramics can be improved when T_{O-T} is shifted to near room temperature [4–7].

Our previous study [8] indicates that the crystal phases and electrical properties of KNN–$LiTaO_3$–$NaSbO_3$ ceramics are influenced by the partial substitution of Sb^{5+} for B-site ions, and the ceramic with 6 mol% $NaSbO_3$ shows good electrical performance due to the coexistence of orthorhombic and tetragonal phases near room temperature. However, the T_C decreases gradually with the increasing $NaSbO_3$ content and the ceramics have a loose microstructure and high porosity. Previous researches have demonstrated that the T_C and T_{O-T} of the KNN-based ceramics can be shifted by the increasing Li content [9,10]. Meanwhile, it is known that Li_2O is usually used as

*Corresponding author at: China University of Geosciences, Faculty of Materials Science and Chemistry, No. 388, Lumo Road, Wuhan 430074, China. Tel.: +86 27 87483374.
E-mail address: y.q.huang@163.com (Y. Huang).

0272-8842/$ - see front matter © 2012 Elsevier Ltd and Techna Group S.r.l. All rights reserved.
http://dx.doi.org/10.1016/j.ceramint.2012.12.086

sintering additive due to its low melting point [11], which will promote the densification of KNN-based ceramics. On the other hand, recent research shows that $K_xNa_{1-x}NbO_3$ ceramics with $x=0.49$ has the peak values of the piezoelectric constant d_{33} of 146 pC/N and the planar electromechanical coupling coefficient k_p of 43% [12]. In order to investigate the effect of Li on the properties of the KNN-based ceramics with sodium-rich compositions, $[(K_{0.49}Na_{0.51})_{1-x}Li_x](Nb_{0.90}Ta_{0.04}Sb_{0.06})O_3$ ($x=0.01$–0.08) ceramics were studied. The crystal phases and electrical properties of the ceramics with different Li content were investigated.

2. Experimental details

$[(K_{0.49}Na_{0.51})_{1-x}Li_x](Nb_{0.90}Ta_{0.04}Sb_{0.06})O_3$ (abbreviated as KNLNTS, $x=0.01$, 0.02, 0.03, 0.04, 0.05, 0.06, 0.08) ceramics were prepared by a conventional ceramics processing route using reagent grade K_2CO_3, Na_2CO_3, Li_2CO_3, Nb_2O_5, Ta_2O_5 and Sb_2O_3 as starting raw materials. The powders were mixed in stoichiometric proportions and milled in ethanol for 12 h, then dried and calcined at 850 °C for 5 h. After the calcination, the powders were reground and mixed with 5 wt% polyvinyl alcohol (PVA) solution as binder, and then uniaxially pressed into discs with 20 mm in diameter and about 1 mm in thickness. The green discs were heated at 650 °C for 5 h to eliminate the binder and finally sintered at 1080–1100 °C for 2 h in air atmosphere. The electrodes were made on the surfaces of the discs by firing silver paste at 600 °C for 10 min. The samples were poled in silicon oil bath at 110 °C for 30 min by applying a dc electric field of 5–6 kV/mm. The piezoelectric properties of the ceramics were measured 24 h after poling.

The crystal phases of the ceramics were investigated by X-ray powder diffraction (XRD) with a Cu Kα radiation (X'Pert PRO). The microstructure of the ceramics was studied by using a scanning electron microscopy (SEM) (JSM-6700F). Dielectric measurements were carried out by the TH2810B LCR Meter and WTC2 system from room temperature to 450 °C. The electromechanical coupling factors, k_p and k_t, were determined by a resonance–antiresonance method using an impedance analyzer (Agilent 4294A). The piezoelectric constant d_{33} was measured by a quasistatic piezoelectric constant testing meter (ZJ-3A). The polarization versus electric field (P–E) hysteresis loops of the ceramics were measured by a Radiant Precision LC Workstation at 10 Hz.

3. Results and discussion

Fig. 1 shows the XRD patterns of the KNLNTS ceramics sintered in air at 1080–1100 °C for 2 h. No secondary phase can be detected when $x \le 0.06$, indicating that Li has completely diffused into the perovskite lattice. However, a trace amount of secondary phase is detected when $x=0.08$. This result reveals that the maximum solid

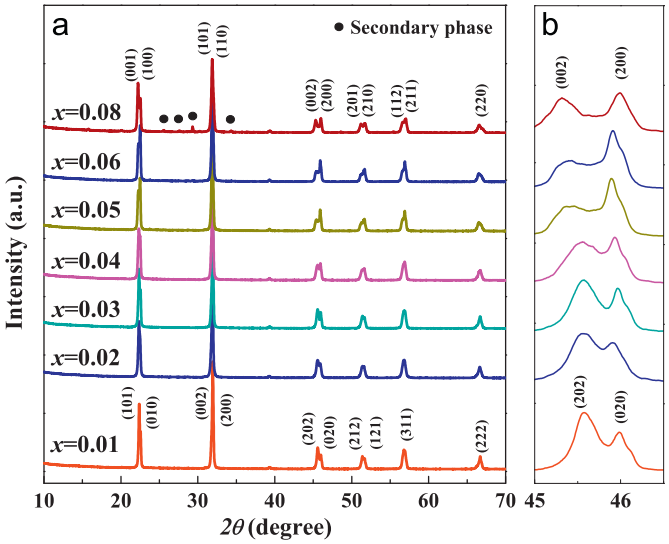

Fig. 1. XRD patterns of the KNLNTS ceramics: (a) wide range, (b) selected regions.

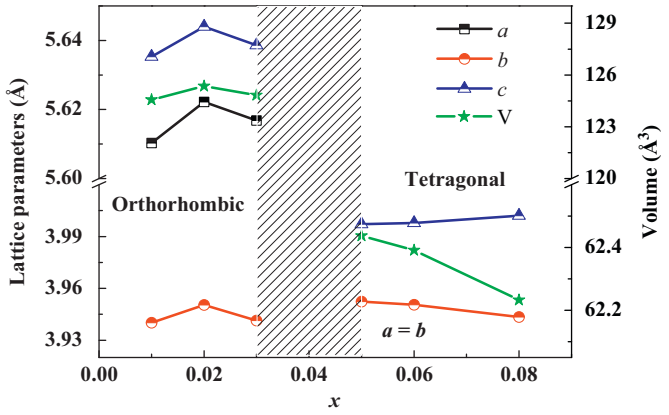

Fig. 2. Lattice parameters and unit cell volume of KNLNTS ceramics.

solubility of lithium in KNLNTS solid solutions is lower than 8 mol%. In addition, XRD patterns show that the crystal structure transforms from orthorhombic to tetragonal as Li content increases. The ceramics with $x \le 0.03$ display an orthorhombic while those with $x > 0.05$ exhibit a tetragonal symmetry. These characteristics suggest that the orthorhombic and tetragonal phases coexist in the ceramics with $0.03 < x < 0.05$. This result means that the polymorphic phase transition temperature (T_{O-T}) of the KNLNTS ceramics can be shifted to near room temperature by increasing Li content.

Fig. 2 shows the lattice parameters and the unit cell volume of the KNLNTS solid solutions with different Li content. It can be seen that the crystal structure is obviously affected by different Li substitution. The lattice parameters change a little with the increasing Li content when the unit cell has orthorhombic symmetry, but when the unit cell becomes tetragonal, the lattice parameters $a=b$ decrease while c increases gradually and the volume of the unit cell decreases obviously with the increasing Li

content. Due to a smaller ionic radius of Li^+ (0.90 Å) than K^+ (1.33 Å) and Na^+ (0.97 Å), substitution of Li^+ for K^+ and Na^+ will lead to crystal distortion and deformation [10]. Similar changes of the unit cell volume of the KNN-based solid solutions can be seen in the systems with the partial substitution of Sb ions for B-site Nb^{5+} ions of the perovskite ABO_3 structure [13]. Sb is a valence-variable element, Sb^{3+} (0.90 Å) and Sb^{5+} (0.62 Å), but many researchers believe that most Sb substituting Nb^{5+} in the modified KNN system are in Sb^{5+} state [3,14–17]. Because the ionic radius of Sb^{3+} is much larger than that of Nb^{5+} (0.69 Å), the Sb^{3+} concentration must be below a certain limit in order to maintain the stability of the perovskite structure. The difference in ionic radius between Sb^{5+} and Nb^{5+} is small. The partial substitution of Sb^{5+} for Nb^{5+} will cause a weak lattice distortion. In addition, the Sb content is maintained at 4 mol% in this work. The crystal structure of the KNN-based solid solution with 4 mol% Sb is similar with that of the pure KNN when Li is not added. Therefore, the decrease of the unit cell volume with the increase of Li content is the result of the crystal distortions and deformation caused by the substitution of Li^+ for K^+ or Na^+ on the A-site.

Fig. 3 shows the SEM micrographs of the fractured surface of the KNLNTS ceramics. It can be seen that the ceramic with $x=0.01$ exhibits a relatively homogonous microstructure with a 1–2 μm grain size (Fig. 2a). As Li content increases, the grains become larger. When 8 mol% Li is added, the size distribution of the grains becomes obviously bimodal, which is about 1–2 μm for the small grains and 4–5 μm for the coarse-grains (Fig. 3d). This phenomenon is probably attributed to the partial remelting and recrystallization due to the good fluxing properties of Li_2O. The partial melting takes place during the sintering process of the ceramics with high Li content. The liquid phase transforms into crystalline phase, which undergoes secondary nucleation and growth during the cooling process. Meanwhile, the liquid phase will accelerate grain growth during the sintering process of the ceramics [18]. Therefore, bimodal grain size distribution is produced in the ceramics with high Li content.

Fig. 4 shows the temperature dependence of the relative permittivity, ε_r, and the loss tangent, tan δ, for the unpoled KNLNTS ceramics at 10 kHz. It can be seen that the dielectric peak corresponding to tetragonal–cubic phase transition (T_C) shifts monotonously to higher temperatures with the increase of Li content. In contrast, the peak corresponding to orthorhombic–tetragonal phase transition (T_{O-T}) shifts gradually to lower temperature with the increasing Li content and disappears for the ceramics with $x \geq 0.05$, indicating the T_{O-T} is lower than room temperature. It means that the ceramics with $x \geq 0.05$ have tetragonal phase at room temperature, which is in accordance with the results of XRD analysis as shown in Fig. 1. The variations of T_C and T_{O-T} of the KNLNTS ceramics with different Li content are summarized in Fig. 5. Because of the high Curie temperature and the large crystal anisotropy of $LiNbO_3$, the increase of T_C should be attributed to $[BO_6]$ octahedral distortion in the ABO_3 perovskite induced by Li substitution [19]. Moreover, the increase of T_C is also considered to be the result of the enhancement of tetragonality [20]. Therefore, the variation

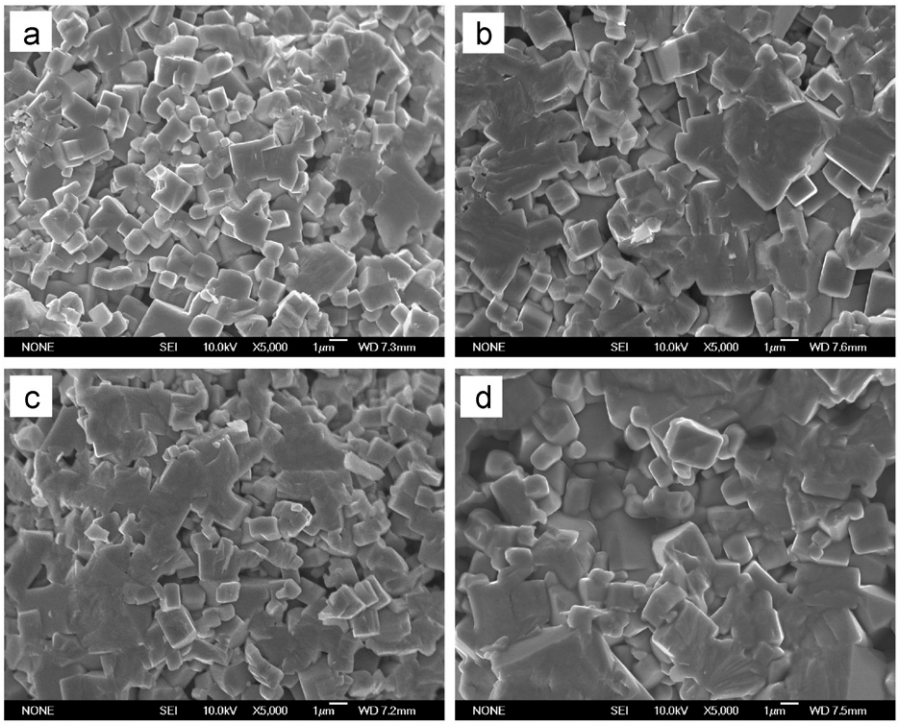

Fig. 3. SEM micrographs of KNLNTS ceramics with different Li content: (a) $x=0.01$, (b) $x=0.03$, (c) $x=0.06$ and (d) $x=0.08$.

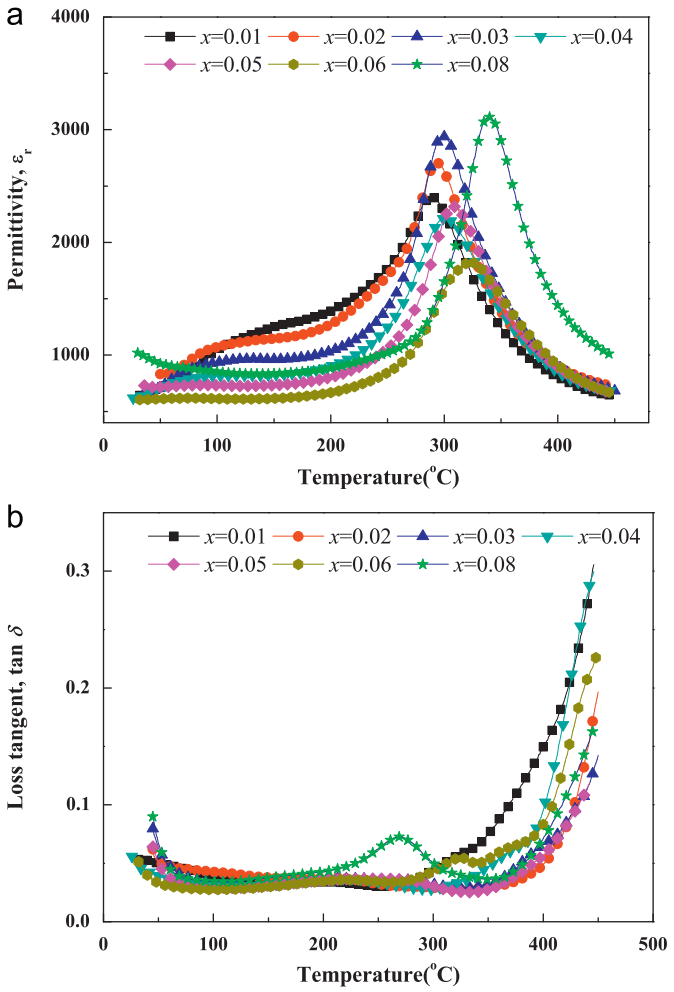

Fig. 4. Temperature dependence of (a) permittivity and (b) loss tangent of KNLNTS ceramics with different Li content at 10 kHz.

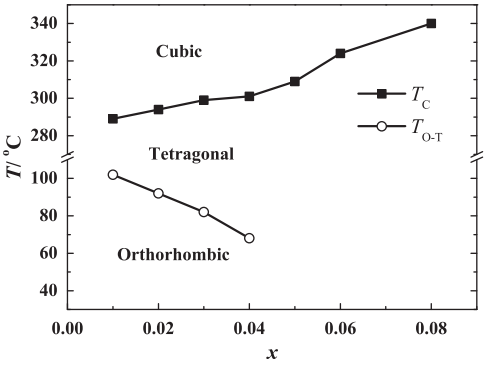

Fig. 5. The T_C and T_{O-T} versus Li content for KNLNTS ceramics.

of T_C is probably ascribed to the changes of the crystal structure induced by Li substitution.

It should be noted that although the ceramic with $x=0.04$ exhibits a coexistence of the orthorhombic and tetragonal phases at room temperature, the T_{O-T} determined in accordance with the peaks of ε_{r-T} curves is higher than room temperature. Zuo et al. have indicated that it is a thermal hysteretic effect during heating when the dielectric constant is measured [21]. Analogously, Gao et al. also pointed out that the state of the ceramics during a heating or cooling process may not always be quasi-equilibrium or equilibrium and the domain structure need a certain amount of time to fulfill the adjustment when it contains coexistent phase [22]. Meanwhile, Peng et al. pointed out that the polymorphic phase transition occurs in a certain temperature range rather than at an exact temperature [23]. Therefore, the phase transition temperature determined according to the ε_{r-T} curves is less accurate and the actual T_{O-T} should be a little lower than that of measurement.

In order to investigate the effect of poling on the T_{O-T} and the dielectric properties, the ε_{r-T} curves of the unpoled and poled ceramic with $x=0.04$ are measured, respectively, as shown in Fig. 6. It can be seen that the T_{O-T} of the ceramics before and after poling keeps unchanged. Moreover, the poled ceramic has a larger dielectric constant than the unpoled sample. Bathelt et al. found that the permittivity of tetragonal phase is larger after poling, while it is smaller to the orthorhombic phase [24]. Chang et al. also reported that the poled $(K_{0.44}Na_{0.52}Li_{0.04})(Nb_{0.80-x}Ta_{0.20}Sb_x)O_3$ ceramics with tetragonal symmetry had larger dielectric constant than the unpoled samples, and the variation of dielectric constants before and after poling became smaller when the distortion of crystal lattice took place [25]. Simultaneously, Wang et al. studied the $K_{0.5}Bi_{4.5}Ti_4O_{15}$ (KBT) compound with orthorhombic symmetry and found that the permittivity of the poled KBT was lower than that of the unpoled KBT [26]. Therefore, the crystal structure of the KNLNTS ceramic $x=0.04$ should be a little closer to tetragonal phase side, even though the T_{O-T} is close to room temperature, which means the coexistence of orthorhombic and tetragonal phases in the ceramic.

In addition, the dielectric peak near T_C is broadened, which is one of the characteristics of the disordered perovskite structure with diffuse phase transition. The diffuseness of the phase transition can be described from the modified Curie–Weiss law $(1/\varepsilon)-(1/\varepsilon_m)=(T-T_m)^{\gamma}/C$ [27], where γ is the degree of diffuseness, ε_m is the

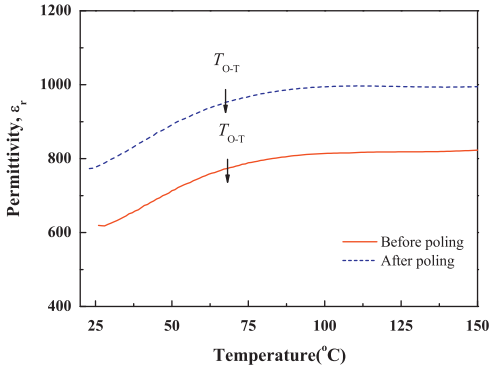

Fig. 6. Temperature dependence of permittivity of the unpoled and poled ceramic with $x=0.04$ at 10 kHz.

maximum dielectric constant, T_m is the temperature at ε_m, and C is the Curie–Weiss constant. γ can be determined by the slope of the graph plotted between $\ln(1/\varepsilon-1/\varepsilon_m)$ versus $\ln(T-T_m)$. The value of γ gives information on the character of the phase transition. $\gamma=1$ is the case for normal ferroelectric, $\gamma=2$ describes to a full relaxor state with completely diffuse phase transition, and $1<\gamma<2$ represents a combined ferroelectric/relaxor state with a certain degree of diffuseness in the phase transition. Fig. 7 shows the plot of $\ln(1/\varepsilon-1/\varepsilon_m)$ as a function of $\ln(T-T_m)$ for KNLNTS ceramics with different Li content. The value of γ is in the range of 1.525–1.719 for KNLNTS ceramics. The highest value, 1.719, of γ is obtained for the ceramic with $x=0.04$, exhibiting the diffuse phase transition behavior.

Fig. 8 shows the electrical properties of KNLNTS ceramics as a function of Li content. As can be seen, d_{33} value increases gradually with the increasing Li content

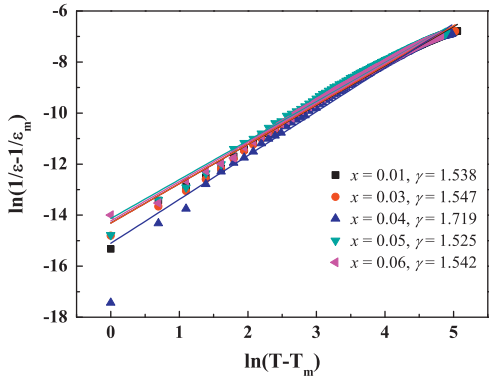

Fig. 7. $\ln(1/\varepsilon-1/\varepsilon_m)$ as a function of $\ln(T-T_m)$ for KNLNTS ceramics.

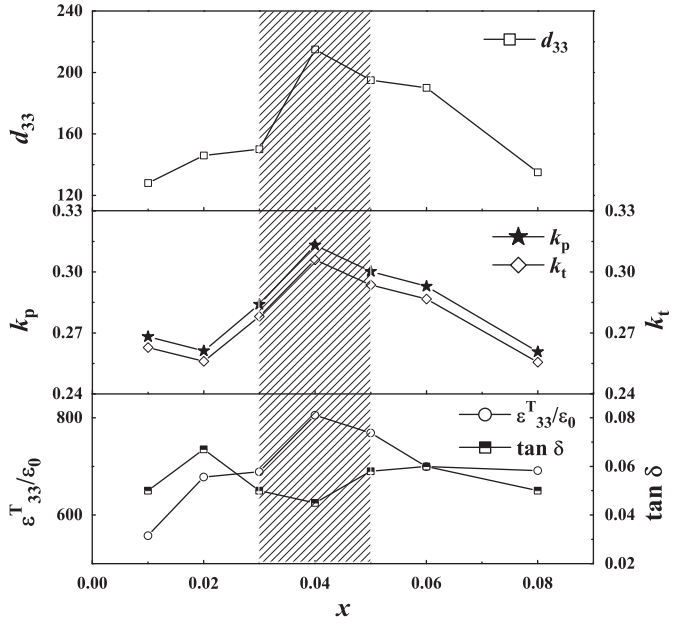

Fig. 8. Piezoelectric constant d_{33}, electromechanical coefficient k_p, k_t, relative permittivity $\varepsilon_{33}^T/\varepsilon_0$ and dielectric loss tan δ of KNLNTS ceramics as a function of x.

when $x\leq 0.04$ and the highest d_{33} value of 215 pC/N is obtained at $x=0.04$. When $x>0.04$, the d_{33} value decreases gradually. The variations of k_p, k_t and $\varepsilon_{33}^T/\varepsilon_0$ with the increase of Li content are much similar to that of d_{33} coefficient. The highest values of k_p, k_t and $\varepsilon_{33}^T/\varepsilon_0$ are 0.313, 0.306 and 805.2, respectively. The ceramics have relatively low tan δ in the range of 0.045–0.067. The lowest value of tan δ is obtained for the ceramic with $x=0.04$. These results indicate that the properties of the ceramics are strongly affected by the crystal structure. As discussed above, when $x=0.04$, a coexistence of the orthorhombic and tetragonal phases is formed, which will make the ferroelectric domain switching occur more easily and enhance substantially the spontaneous polarization.

4. Conclusions

$[(K_{0.49}Na_{0.51})_{1-x}Li_x](Nb_{0.90}Ta_{0.04}Sb_{0.06})O_3$ ($x=0.01$, 0.02, 0.03, 0.04, 0.05, 0.06, 0.08) ceramics were fabricated by a conventional ceramic fabrication technique. A secondary phase was identified by XRD analysis when $x=0.08$, indicating that the maximum solid solubility of lithium in KNLNTS solid solutions is lower than 8 mol%. The Curie temperature T_C increases while the phase transition temperature T_{O-T} decreases with the increasing Li content. The coexistence of the orthorhombic and tetragonal phases was formed in the ceramic with $x=0.04$ at room temperature. The optimum electrical performance, i.e. $d_{33}=215$ pC/N, $k_p=0.313$, $k_t=0.306$, $\varepsilon_{33}^T/\varepsilon_0=805$ and tan $\delta=0.045$, was obtained for $x=0.04$.

Acknowledgments

This work was supported by the Open Foundation of Teaching Laboratory of China University of Geosciences, China (No. SKJ2011117).

References

[1] L. Egerton, D.M. Dillom, Piezoelectric and dielectric properties of ceramics in the system potassium–sodium niobate, Journal of the American Ceramic Society 52 (1959) 438–442.

[2] H. Birol, D. Damjanovic, N. Setter, Preparation and characterization of $(K_{0.5}Na_{0.5})NbO_3$ ceramics, Journal of the European Ceramic Society 26 (2006) 861–866.

[3] Y. Saito, H. Takao, T. Tani, T. Nonoyama, K. Takatori, T. Homma, T. Nagaya, M. Nakamura, Lead-free piezoceramics, Nature 432 (2004) 84–87.

[4] E.K. Akdoğan, K. Kerman, M. Abazari, A. Safari, Origin of high piezoelectric activity in ferroelectric $(K_{0.44}Na_{0.52}Li_{0.04})Nb_{0.84}Ta_{0.1}Sb_{0.06})O_3$ ceramics, Applied Physics Letters 92 (2008) 112908–112910.

[5] J.L. Zhang, X.J. Zong, L. Wu, Y. Gao, P. Zheng, S.F. Shao, Polymorphic phase transition and excellent piezoelectric performance of $(K_{0.55}Na_{0.45})_{0.965}Li_{0.035}Nb_{0.80}Ta_{0.20}O_3$ lead-free ceramics, Applied Physics Letters 95 (2009) 022909–022911.

[6] Y.S. Sung, J.H. Lee, S.W. Kim, T.H. Lee, J.M. Kim, J.H. Cho, T.K. Song, M.H. Kim, T.G. Park, Enhanced piezoelectric properties of $(Na_{0.53}K_{0.47})(Nb_{1-x}Ta_x)O_3$ ceramics by Ta substitution, Ceramics International 38S (2012) S301–S304.

[7] G.Z. Zang, J.F. Wang, H.C. Chen, W.B. Su, C.M. Wang, P. Qi, B.Q. Ming, J. Du, L.M. Zheng, S.J. Zhang, T.R. Shrout, Perovskite $(Na_{0.5}K_{0.5})_{1-x}(LiSb)_xNb_{1-x}O_3$ lead-free piezoceramics, Applied Physics Letters 88 (2006) 212908–212910.

[8] H.W. Du, Y.Q. Huang, H.L. Li, H.P. Tang, W. Feng, Effects of $NaSbO_3$ on phase structure and electrical properties of $K_{0.5}Na_{0.5}NbO_3$–$LiTaO_3$–$NaSbO_3$ piezoelectric ceramics, Journal of Materials Science: Materials in Electronics (2012)http://dx.doi.org/10.1007/s10854-012-0834-2.

[9] Y.P. Guo, K. Kakimoto, H. Ohsato, Phase transitional behavior and piezoelectric properties of $Na_{0.5}K_{0.5}NbO_3$–$LiNbO_3$ ceramics, Applied Physics Letters 85 (2004) 4121–4123.

[10] S. Wongsaenmai, S. Ananta, R. Yimnirun, Effect of Li addition on phase formation behavior and electrical properties of $(K_{0.5}Na_{0.5})NbO_3$ lead free ceramics, Ceramics International 38 (2012) 147–152.

[11] J. Fu, R.Z. Zuo, D.Y. Lv, Y. Liu, Y. Wu, Structure and piezoelectric properties of lead-free $(Na_{0.52}K_{0.442-x})(Nb_{0.952-x}Sb_{0.05})O_{3-x}LiTaO_3$ ceramics, Journal of Materials Science: Materials in Electronics 21 (2010) 241–245.

[12] Y.M. Li, Z.Y. Shen, L. Jiang, R.H. Liao, Z.M. Wang, Y. Hong, Microstructure, phase transition, and electrical properties of $K_xNa_{1-x}NbO_3$ lead-free piezoceramics, Journal of Electronic Materials 41 (2012) 546–551.

[13] H.E. Mgbemere, G.A. Schneider, T.A. Stegk, Effect of antimony substitution for niobium on the crystal structure, piezoelectric and dielectric properties of $(K_{0.5}Na_{0.5})NbO_3$ ceramics, Functional Materials Letters 3 (2010) 25–30.

[14] J. Du, J.F. Wang, G.Z. Zang, P. Qi, S.J. Zhang, T.R. Shrout, $Na_{0.52}K_{0.44}Li_{0.04})Nb_{0.9-x}Sb_xTa_{0.1}O_3$ lead-free piezoelectric ceramics with high performance and high Curie temperature, Chinese Physics Letters 25 (2008) 1446–1448.

[15] R.Z. Zuo, J. Fu, D.Y. Lv, Y. Liu, Antimony tuned rhombohedral–orthorhombic phase transition and enhanced piezoelectric properties in sodium potassium niobate, Journal of the American Ceramic Society 93 (2010) 2783–2787.

[16] D.M. Lin, K.W. Kwok, K.H. Lam, H.L.W. Chan, Structure and electrical properties of $K_{0.5}Na_{0.5}NbO_3$–$LiSbO_3$ lead-free piezoelectric ceramics, Journal of Applied Physics 101 (2007) 074111–074116.

[17] B.Q. Ming, J.F. Wang, P. Qi, G.Z. Zang, Piezoelectric properties of (Li,Sb,Ta) modified $(Na,K)NbO_3$ lead-free ceramics, Journal of Applied Physics 101 (2007) 054103–054106.

[18] Y.H. Zhen, J.F. Li, Abnormal grain growth and new core-shell structure in $(K,Na)NbO_3$–based lead-free piezoelectric ceramics, Journal of the American Ceramic Society 90 (2007) 3496–3502.

[19] M. Matsubara, T. Yamaguchi, K. Kikuta, S. Hirano, Effect of Li substitution on the piezoelectric properties of potassium sodium niobate ceramics, Japanese Journal of Applied Physics 44 (2005) 6136–6142.

[20] J. Fu, R.Z. Zuo, X.S. Fang, K. Liu, Lead-free ceramics based on alkaline niobate tantalate antimonate with excellent dielectric and piezoelectric properties, Materials Research Bulletin 44 (2009) 1188–1190.

[21] R.Z. Zuo, J. Fu, X.H. Wang, L.T. Li, Phase transition and domain variation contributions to piezoelectric properties of alkaline niobate based lead-free systems, Journal of Materials Science: Materials in Electronics 21 (2010) 519–522.

[22] Y. Gao, J.L. Zhang, Y.L. Qing, Y.Q. Tan, Z. Zhang, X.P. Hao, Remarkably strong piezoelectricity of lead-free $(K_{0.45}Na_{0.55})_{0.98}Li_{0.02}(Nb_{0.77}Ta_{0.18}Sb_{0.05})O_3$ ceramic, Journal of the American Ceramic Society 94 (2011) 2968–2973.

[23] B. Peng, Z.X. Yue, L.T. Li, Evaluation of domain wall motion during polymorphic phase transition in $(K,Na)NbO_3$-based piezoelectric ceramics by nonlinear response measurements, Journal of Applied Physics 109 (2011) 054107–054112.

[24] R. Bathelt, T. Soller, K. Benkert, C. Schuh, A. Roosen, Neodymium doping of KNNLT, Journal of the European Ceramic Society 32 (2012) 3767–3772.

[25] Y.F. Chang, Z.P. Yang, L.R. Xiong, Z.H. Liu, Z.L. Wang, Phase Structure, microstructure, and electrical properties of Sb-modified $(K,Na,Li)(Nb,Ta)O_3$ piezoelectric ceramics, Journal of the American Ceramic Society 91 (2008) 2211–2216.

[26] C.M. Wang, J.F. Wang, Aurivillius phase potassium bismuth titanate: $K_{0.5}Bi_{4.5}Ti_4O_{15}$, Journal of the American Ceramic Society 91 (2008) 918–923.

[27] K. Uchino, S. Nomura, Critical exponents of the dielectric constants in diffused-phase-transition crystals, Ferroelectrics Letters 44 (1982) 55–61.